Delft University of Technology

Delft Center for Systems and Control

Technical report 23-014

Predictive control of a human-in-the-loop network system considering operator comfort requirements*

A.D. Sadowska, J.M. Maestre, R. Kassing, P.J. van Overloop, and
B. De Schutter

---

* This report can also be downloaded via https://pub.bartdeschutter.org/abs/23_014.html

Predictive Control of a Human-in-the-loop Network System Considering Operator Comfort Requirements

A.D. Sadowska, J.M. Maestre, R. Kassing, P.J. van Overloop, and B. De Schutter

Abstract—We propose a model-predictive control (MPC)-based approach to solve a human-in-the-loop control problem for a network system lacking sensors and actuators to allow for a fully automatic operation. The humans in the loop are therefore essential; they travel between the network nodes to provide the remote controller with measurements and to actuate the system according to the controller's commands. Time instant optimists MPC is utilized to compute when the measurement and actuation actions are to take place to coordinate them with the network dynamics. The time instants also minimize the burden of human operators by tracking their energy levels and scheduling the necessary breaks. Fuel consumption related to the operators' travel is also minimized. The results in a digital twin of the Dez Main Canal illustrate that the new algorithm outperforms previous methods in terms of meeting operational objectives and taking care of human well-being, but at the cost of higher computational requirements.

Index Terms—MPC, human-in-the-loop, network systems

I. INTRODUCTION

The optimal operation of large-scale networked systems can require a significant amount of automation, but the cost of installing and maintaining the corresponding sensors, actuators, and the communication infrastructure can become prohibitive. A cost-effective alternative observed in many real-life applications is to have human operators traveling between various parts of the system to take measurements and provide actuation as they see fit, avoiding or minimizing the use of sensors and actuators. Irrigation canals management is a well-known example in this regard due to the high setup and maintenance costs, and the problems of theft and vandalism, for automatic equipment is installed and left unattended. Although multiple automatic methods have been proposed [1], it is still common to resort to manual control so that a human operator travels along the canal, changing gates settings as he or she deems appropriate.

Nevertheless, it is still possible to design advanced control methods based on the employment of human operators to measure [2, 3] and act within the system to improve performance. For example, the case of irrigation canals is explicitly considered in [4]. A similar concept is explored in [5], where

A.D. Sadowska is with Schlumberger Cambridge Research, Cambridge, United Kingdom; J.M. Maestre is with the Department of Systems and Automation Engineering, University of Seville, Spain, and with the Department of Systems Science, Kyoto University, Japan; R.C. Kassing is with the Water Resources Management section, Delft University of Technology, The Netherlands; P.-J. van Overloop was with the Water Resources Management section, Delft University of Technology, The Netherlands; B. De Schutter is with the Delft Center for Systems and Control, Delft University of Technology, The Netherlands; (e-mail: ASadowska@slb.com).

the controller provides the human with a set of admissible control actions that he or she is allowed to choose from. Indeed, this is often the case of decision support systems [6], which drive operator decisions, although they can occasionally be overruled based on human expertise.

As a matter of fact, the entanglement between automation and humans is anything but exceptional, especially since many control systems are specifically designed to satisfy human needs. Typical examples include the control of vehicles [7, 8], exoskeletons [9] and groups of robots [10, 11], rehabilitative robotics [12, 13], and bilateral teleoperation [14]. To this end, a wide variety of approaches are employed, e.g., reference models [15]; formal methods [16] to satisfy the required control specifications; model predictive control (MPC) to compute operator actions [6, 17] and model his or her control law [18]; Markov models to describe human behavior [19]; and a family of feedback methods to obtain references, e.g., via touchscreens [11] and haptic interfaces [20], and also learn from the human, e.g., via physiological measurements [12, 21] and ratings [13]. Furthermore, research also explores topics such as fatigue detection in pilots [22], the minimization of cognitive overload [23], and human tendencies, e.g., to anticipate commands [24] and minimize efforts [18, 25], operator properties such as passivity to obtain stability guarantees [26], and even human biases, e.g., overconfidence [27]. Finally, in the context of large-scale systems operated by humans, we also note similarities between the underlying problem of finding a route for an operator and the asset routing problem [28] as well as the visit scheduling problem for target patrolling [29]. In this regard, the issue of explicitly considering human factors was discussed in [30].

The specific human-in-the-loop problem we deal with was first studied in [17, 31], which introduced the so-called mobile model predictive control (MoMPC) approach,[1] where human operators travel between various locations of an irrigation canal taking measurements and following the instructions provided by a centralized MPC controller in an event-driven fashion. In particular, the operator communicates new measurements from a visited location to the controller using a mobile device, and in return receives the control actions to be applied as well as the next location to go to, which is computed accounting for the travel time between different locations and the time needed at a local site. In [32], the MoMPC framework was enhanced using time instant optimization MPC (TIO-MPC) [33, 34]. Unlike [17, 31], where actuation instants follow directly from the travel times of the route computed, TIO-MPC

---

[1]MoMPC is a patented technology that is commercialized by Mobile Water Management. More information at https://mobilewatermanagement.nl.

allows the controller to freely determine these time instants subject to operational constraints, e.g., to introduce waiting periods that synchronize the operator action with the system dynamics, thus enhancing performance [32].

In previous works [17, 31, 32], the case of multiple operators was simplified by optimizing the route and control actions of one operator at a time (with the schedules of other operators kept constant) [17]. Here, we propose a generic multi-operator problem where the schedules for all operators are computed based on a more realistic transportation infrastructure, where multiple routes, time-of-day-dependent travel times, and fuel consumption are considered. Given the highly scarce nature of the measuring and actuating actions that the operator can provide in a large-scale system, the controller is given the freedom to schedule both when the measurement is taken and the exact time instants at which the control action is applied. Also, to enhance the information gathering, we add a new penalty that encourages the controller to assign operator visits evenly, so that all parts of the system can be monitored even in the absence of fixed remote sensors. Finally, we consider novel human-related aspects to improve human operators' well-being, e.g., stress levels and scheduling of breaks.

The outline of this article is as follows. In Section II, we define the network system and the internal model of the controller. In Section III, the objectives weighted by the controller and the optimization problem solved are given. The performance of the controller is illustrated in Section IV using the Dez canal in Iran as a case study. Finally, conclusions and future directions are given in Section V.

II. Network system modeling

We consider a network system described by a graph $\mathcal{G} = (\mathcal{V}, \mathcal{E})$. Here $\mathcal{V}$ is the set of nodes (i.e. all measurement and actuating locations in the network system[2]) and $\mathcal{E}$ denotes the set of edges of the graph such that $(v_i, v_j) \in \mathcal{E}$ if there is a direct route between nodes v_i and v_j in $\mathcal{G}$ [35].

Define a set of all admissible routes in the network from node v_i to node v_j as

$$\mathcal{R}_{v_i \to v_j} = \left\{ \mathcal{R}^1_{v_i \to v_j}, \ldots, \mathcal{R}^{N_{\text{routes}, v_i \to v_j}}_{v_i \to v_j} \right\}. \quad (1)$$

Each individual route $\mathcal{R}^c_{v_i \to v_j}$, $c = 1, \ldots, N_{\text{routes}, v_i \to v_j}$ is associated with a specific distance $\mathcal{D}^c_{v_i \to v_j}$ that must be traveled by the operator along that route. It is required that there are no cycles on the routes and that the distance of each route $\mathcal{R}^c_{v_i \to v_j}$ is bounded, i.e., $\mathcal{D}^c_{v_i \to v_j} \leq \mathcal{D}_{\text{max}}$. Furthermore, assume that each path $\mathcal{R}^c_{v_i \to v_j}$ is associated with a certain operator stress level $\mathcal{S}^c_{j, v_i \to v_j} \in (0, 1)$ per time unit and is assigned an average time-varying speed $v^c_{v_i \to v_j}(t)$ with which one travels along this route. Variations between stress levels and average speed for different routes between two nodes could stem from a different nature of different routes, e.g. one route may be a calm, rural road and another may be a highway with different traffic conditions depending on the time of the day (i.e., at peak and off-peak times).
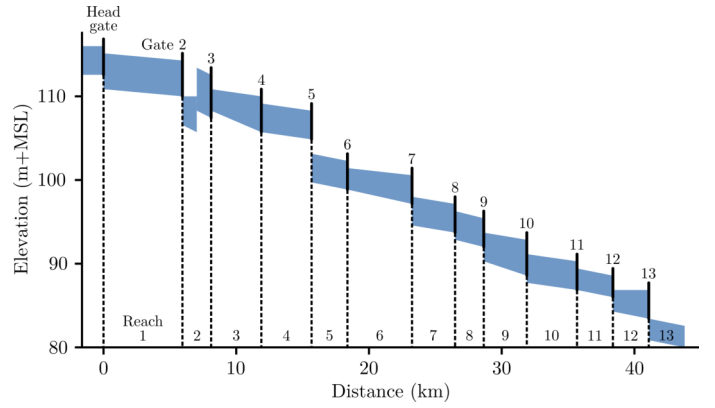

Figure 1. Longitudinal profile of Dez canal. Due to the elevation with respect to mean sea level (MSL), water flows downstream along its more than 40 kilometers length. The canal is composed of 13 sections separated by gates that can be adjusted manually to regulate flows and water levels.

To calculate the instants of time of the operators' actions, we consider a network with $|\mathcal{V}| = N$ nodes and employ the continuous-time model[3]

$$\dot{x}(t) = Ax(t) + B_{\text{u}}u(t) + B_{\text{d}}d(t) + w(t), \quad (2)$$

$$y(t) = H(t)x(t) + v(t), \quad (3)$$

where $x(t) \in \mathbb{R}^n$ denotes the state, $u(t) \in \mathbb{R}^m$ denotes the input, $d(t) \in \mathbb{R}^r$ denotes the known exogenous input, $w(t) \in \mathbb{R}^n$ denotes the unknown process noise, $y(t) \in \mathbb{R}^p$ denotes the measured output, and $v(t) \in \mathbb{R}^p$ is the unknown measurement noise. The overall state and control input vectors can be written as $x(t) = \left(x_1^{\text{T}}(t), \ldots, x_N^{\text{T}}(t) \right)^{\text{T}}$ and $u(t) = \left(u_1^{\text{T}}(t), \ldots, u_N^{\text{T}}(t) \right)^{\text{T}}$, and they are subject to operational constraints, i.e., $x(t) \in \mathcal{X}$ and $u(t) \in \mathcal{U}$, where $\mathcal{X}$ and $\mathcal{U}$ are nonempty sets.

For example, consider the case of an irrigation canal (see Figure 1). Here, $x(t)$ is a vector containing the deviations of water levels with respect to their setpoints (i.e., regulation errors) and possibly delayed flows of the 13 nodes of the canal, $u(t)$ typically represents increments in water flows due to changes in the operating infrastructure (e.g, the position of gates), $d(t)$ contains exogenous inputs such as the manipulation of offtakes by farmers to take water, and $w(t)$ and $v(t)$ are disturbances that model issues such as rainfall runoff, evaporation, and instrument noise. Therefore, $x_i(t)$ and $u_i(t)$ refer to these magnitudes at the node $i \in \mathcal{V}$ of the canal, which are relevant to the local dynamics of the corresponding section. Also, sets $\mathcal{X}$ and $\mathcal{U}$ contain the set of admissible values for the previously mentioned magnitudes, e.g., maximum and minimum water levels and flows. Finally, the matrices A, B_u, B_d and $H(t)$ can be calibrated using identification methods or follow a mechanistic structure as in integrator-delay models [38].

Remark 1: The output matrix $H(t)$ changes over time depending on how many operators are at the measurement nodes at a given time. Specifically, an operator at one of the

---

[2]It is assumed that at each node both measurements can be taken and actuations can be applied. However, the method can be easily extended to accommodate measurement or actuation only nodes.

[3]Models of this kind can be found in the literature for different systems, e.g. for traffic systems in [36] and for irrigation systems in [37].

nodes can provide measurements of the corresponding output. Consequently, $H(t)$ may be an empty matrix when at a given time none of the operators are at any of the measurement nodes. Therefore, the system observability is not ensured. In addition, due to the noise terms $w(t)$ and $v(t)$, the controller requires state estimates (cf. [39]), which can be obtained, e.g., using Kalman filters [40], observers based on Takagi-Sugeno models [41], and moving horizon estimators [42]. In particular, the observer must fuse the measurements obtained by the operators in unevenly spaced sampling steps (cf. [43]). However, our problem setup is designed for systems that are *currently* operated manually. In this regard, a system must possess certain facilitating conditions to be directly controlled by human operators. For example, irrigation canals are passive systems with very slow dynamics. Likewise, as discussed in [44], the loose coupling between canal sections can be exploited to generate decentralized observers with bounded uncertainty. Finally, the reader is referred to works such as [45, 46] and the references therein for a proper discussion of the technical challenges with regard to observability in switching linear systems.

III. CONTROL ALGORITHM

Following [32], we use TIO-MPC [33, 34, 47] to explicitly consider as optimization variables the time instants of measurements and actuations.[4] In comparison to the original MoMPC [17, 31], the arrival and actuation time instants no longer follow from fixed traveling times between locations, i.e., the operator may have some waiting periods to synchronize the measuring and actuating processes with the system dynamics to improve performance. In the current setup with human operators, the resulting control algorithm is named Time Instant Optimization MoMPC (TIO-MoMPC).

A. Route definition

Consider a network with $N_{\mathrm{op}} \geq 1$ operators indexed by $j \in \mathcal{O} := \{1, \dots, N_{\mathrm{op}}\}$. Given an activation time $\breve{t} \in \mathbb{R}$ of the proposed event-driven control strategy, a subset of operators $\breve{\mathcal{O}}(\breve{t}) \subseteq \mathcal{O}$ are considered available to take and communicate measurements from their current locations, and receive information on what actions to apply. Thus, operators $j \notin \breve{\mathcal{O}}(\breve{t})$ are either traveling or completing some activities. We define a travel status function for operators $j \notin \breve{\mathcal{O}}(\breve{t})$ as

$$\mathrm{st}_j(\breve{t}) = \begin{cases} 1 & \text{if operator } j \text{ is traveling,} \\ 0 & \text{otherwise.} \end{cases} \quad (4)$$

It is assumed that traveling operators must go to the next location that they were originally assigned to, but the remainder of their trip can be altered. Those operators that are completing some activities at a location, need to be allowed $T_{\mathrm{busy},j}(\breve{t})$ time units to finish the activities before new instructions can be given to them. Since they have not yet departed en-route, they can be given a completely new schedule by the controller once they are free.

Define the path variable for the operator j as $p_j(\breve{t}) = (p_{1,j}(\breve{t}), \dots, p_{N_{\mathrm{s}},j}(\breve{t}))$, $p_{\ell,j}(\breve{t}) \in \mathcal{V}$, which contains the N_{s} consecutive indices of nodes to be visited by the operator, in which $p_{1,j}(\breve{t}) = v_{\mathrm{current},j}(\breve{t})$ (the current node visited) for $j \in \breve{\mathcal{O}}(\breve{t})$, and $p_{1,j}(\breve{t}) = p_{1,j}(\breve{t}_{\mathrm{prev}})$ for $j \notin \breve{\mathcal{O}}(\breve{t})$ if $\mathrm{st}_j(\breve{t}) = 1$, where $\breve{t}_{\mathrm{prev}}$ denotes the time of the preceding activation of the controller. The elements of the path variable $p_j(\breve{t})$ may be repeated, as it may be worthwhile for an operator j to inspect and actuate a subset of possible locations more than once. However, we will later introduce a penalty term (cf. (8)) in the cost function of the model predictive controller to stimulate all locations to be visited regularly to prevent growing uncertainty about some parts of the system. This helps to obtain recurrent measurements from all locations whenever possible, as there is no other means of monitoring the local sites.

For $N_{\mathrm{routes},p_{\ell,j}(\breve{t}) \to p_{\ell+1,j}(\breve{t})} \geq 0$ routes between any two subsequent nodes $p_{\ell,j}(\breve{t})$ and $p_{\ell+1,j}(\breve{t})$ on the operator's route $p_j(\breve{t})$, as an additional degree of freedom, the controller also assigns what specific route the operator should follow between $p_{\ell,j}(\breve{t})$ and $p_{\ell+1,j}(\breve{t})$. To this end, we define a route index variable $r_j(\breve{t})$ such that each element $r_{\ell,j}(\breve{t}) \in \{1, \dots, N_{\mathrm{routes},p_{\ell,j}(\breve{t}) \to p_{\ell+1,j}(\breve{t})}\}$ of $r_j(\breve{t})$ determines the index of the selected admissible route between $p_{\ell,j}(\breve{t})$ and $p_{\ell+1,j}(\breve{t})$, i.e. $r_{\ell,j}(\breve{t})$ is the index c of $\mathcal{R}^c_{p_{\ell,j}(\breve{t}) \to p_{\ell+1,j}(\breve{t})}$.

We denote by $T_j^{\mathrm{meas}}(\breve{t}) = (T_{1,j}^{\mathrm{meas}}(\breve{t}), \dots, T_{N_{\mathrm{s}},j}^{\mathrm{meas}}(\breve{t}))$, $T_{\ell,j}^{\mathrm{meas}}(\breve{t}) \in \mathbb{R}$, the time instants at which the operator j should take measurements at the consecutive locations of the path $p_j(\breve{t})$. Similarly to the first element of the sequence $p_j(\breve{t})$, for $j \in \breve{\mathcal{O}}(\breve{t})$ the first element of $T_j^{\mathrm{meas}}(\breve{t})$ is fixed to the current time $T_{1,j}^{\mathrm{meas}}(\breve{t}) = \breve{t}$. Next, denote the time instants in which the operator j should apply the actuation at the visited locations by $T_j^{\mathrm{act}}(\breve{t}) = (T_{1,j}^{\mathrm{act}}(\breve{t}), \dots, T_{N_{\mathrm{s}},j}^{\mathrm{act}}(\breve{t}))$, $T_{\ell,j}^{\mathrm{act}}(\breve{t}) \in \mathbb{R}$. Unlike $T_j^{\mathrm{meas}}(\breve{t})$, the first element of which is fixed, all elements of $T_j^{\mathrm{act}}(\breve{t})$ are assigned by the controller.

The control actions that the operators apply are, in a general case, defined on a continuous domain to allow the associated control input to be modified continuously. However, in some applications, it may be reasonable to restrict the domain to integers only when the control actions relate to switching the equipment according to its discrete settings (e.g. on/off). We denote the control actions to be executed by the operator j on path $p_j(\breve{t})$ by $u_j^{\mathrm{op}}(\breve{t}) = (u_{1,j}^{\mathrm{op}}(\breve{t}), \dots, u_{N_{\mathrm{s}},j}^{\mathrm{op}}(\breve{t}))$, $u_{\ell,j}^{\mathrm{op}}(\breve{t}) \in \mathbb{R}$. Similarly to $T_j^{\mathrm{act}}(\breve{t})$, this whole sequence is computed given the up-to-date measurements provided by the operator.

With the help of the variables $p_j(\breve{t})$, $T_j^{\mathrm{meas}}(\breve{t})$, $T_j^{\mathrm{act}}(\breve{t})$, and $u_j^{\mathrm{op}}(\breve{t})$ for all $j \in \mathcal{O}$, the trajectories of the control input $u(\cdot)$ are formulated for the duration of the prediction window T_{p}, i.e. from the current activation time $\breve{t}$ until the end of the prediction window $\breve{t} + T_{\mathrm{p}}$. This results in the following relation for $\tau \in [\breve{t}, \breve{t} + T_{\mathrm{p}}]$:

$$u_i(\tau | \breve{t}) = \begin{cases} u_{\ell,j}^{\mathrm{op}}(\breve{t}) \delta(\tau - T_{\ell,j}^{\mathrm{act}}(\breve{t})) & \text{if } v_i = p_{\ell,j}(\breve{t}), \\ 0 & \text{otherwise,} \end{cases} \quad (5)$$

in which δ denotes the Dirac impulse function. Therefore, the operator should communicate to the controller the measurements taken at location $p_{\ell,j}(\breve{t})$ at time $T_{\ell,j}^{\mathrm{meas}}(\breve{t})$. Then, at time

$T_{\ell,j}^{\mathrm{act}}(\check{t})$, the control action $u_{\ell,j}^{\mathrm{op}}(\check{t})$ should be applied at that location. After that, the operator proceeds to the next location $p_{\ell+1,j}(\check{t})$.

To complement the continuous-time dynamics of the network (2)-(3), we use continuous sampled-data MPC [48, 49]. It uses a continuous-time model of a system, but measurements are taken from the system and new control actions are applied only at consecutive sampling times (as opposed to continuously). In our framework, the use of sampled-data MPC enables us to define the time instants $T_j^{\mathrm{meas}}(\check{t})$ and $T_j^{\mathrm{act}}(\check{t})$ as real-valued variables.

Assuming that the estimate $\hat{x}(t)$ is at hand, we characterize the performance of the system by the cost function

$$J_{\mathrm{MoMPC}}(\check{t}) = \int_{\check{t}}^{\check{t}+T_{\mathrm{p}}} \left(\hat{x}^{\mathsf{T}}(\tau|\check{t})Q\hat{x}(\tau|\check{t}) + u^{\mathsf{T}}(\tau|\check{t})Ru(\tau|\check{t}) \right) \mathrm{d}\tau, \tag{6}$$

where Q and R are positive semi-definite matrices. Here, we use a simple quadratic cost function, but more specialized non-linear cost functions can easily be used.

For example, in the irrigation canal example, Q and R are typically diagonal matrices so that cost (6) integrates squared regulation errors and changes in the infrastructure. In this way, the control designer can balance the trade-off between regulation accuracy and control effort, which is related to the lifetime of actuators, by tuning these weight matrices.

Remark 2: From a practical viewpoint, one could use the state of a digital twin of the irrigation canal as a proxy of the real state (e.g., after setting the canal and the digital twin at a certain operation point) and then update the digital twin with the actions implemented and the measurements sent by the operators. Although this practical procedure would introduce uncertainty, the MPC framework has alternatives to deal with this issue, e.g., robust and stochastic formulations [50–52].

B. Network monitoring

Based on the concepts of node refresh time [53] and node idleness [54], we promote regular visits to all locations by adding a penalty $J_{\mathrm{loc}}(t)$, which grows with the time since each location was visited for the last time, see Figure 2. To this end, let us define for each $v_i \in \mathcal{V}$ the elapsed time as

$$\Delta t_i(\tau|\check{t}) = \begin{cases} 0 & \text{if } \tau = T_{\ell,j}^{\mathrm{meas}}(\check{t}) \wedge v_i = p_{\ell,j}(\check{t}), \\ \tau - t_i^{\mathrm{last}}(\tau|\check{t}) & \text{otherwise,} \end{cases} \tag{7}$$

where $t_i^{\mathrm{last}}(\tau|\check{t})$ represents the last time instant that node $v_i \in \mathcal{V}$ is visited by the operator within the time horizon $[\check{t}, \check{t}+T_{\mathrm{p}}]$ according to the computations performed at activation time $\check{t}$. At every new controller activation in response to operator measurements from a location at time $\check{t}$, the initial value is $t_i^{\mathrm{last}}(\check{t}|\check{t}) = t_i^{\mathrm{last}}(\check{t}|\check{t}_{\mathrm{prev}})$, in which $\check{t}_{\mathrm{prev}}$ denotes the activation time immediately before $\check{t}$. The resulting cost function $J_{\mathrm{loc}}(\check{t})$ takes the form

$$J_{\mathrm{loc}}(\check{t}) = \sum_{i=1}^{N} \int_{\check{t}}^{\check{t}+T_{\mathrm{p}}} \alpha_{\mathrm{loc},i}\Delta t_i(\tau|\check{t})\mathrm{d}\tau, \tag{8}$$

in which $\alpha_{\mathrm{loc},i} > 0$ put more or less priority on visiting certain locations as needed. A weighted-sum strategy is used
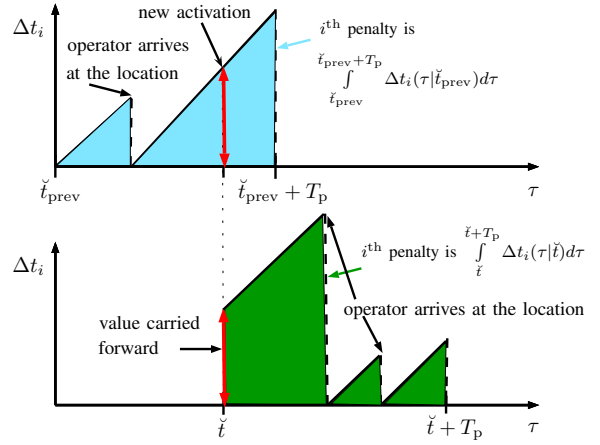

Figure 2. Definition of the variables $\Delta t_i(\tau|t)$. The ith component of the penalty $J_{\mathrm{loc}}(\check{t}_{\mathrm{prev}})$ (($\check{t}$), respectively) represents the blue (green, respectively) area shown.

(cf. (17)) to integrate (8) with other cost components, whereby the minimization of (8) aims at stimulating the controller to take frequent measurements at all locations. On the other hand, it can also bring subsequent time instants closer, which could diminish performance in terms of cost $J_{\mathrm{MoMPC}}(t)$. Therefore, careful selection of the weights (see (17)) of the individual components in the overall cost function is crucial.

In addition to the current persistent monitoring condition, in settings with asynchronous and distributed sampling, the scheduling mechanism could also directly minimize the state estimation error. To this end, one could consider a penalty such as $J_{\mathrm{estimate}}(\check{t}) = \sum_{i=1}^{N} \int_{\check{t}}^{\check{t}+T_{\mathrm{p}}} \beta_{\mathrm{loc},i}\|H(\tau|\check{t})\hat{x}(\tau|\check{t}) - y(\tau|\check{t})\|^2\mathrm{d}\tau$, where $\beta_{\mathrm{loc},i} > 0$. Additionally, the weighting parameters $\alpha_{\mathrm{loc},i}$ and $\beta_{\mathrm{loc},i}$ could be made time-varying or adaptive to the state estimation error. Such extensions are beyond the scope of the present article. The reader is referred to [55] for more details.

C. Operator-centric approach

In contrast to the previous results in [17, 31, 32], where the average travel speed of the human operator was assumed to be constant all the time, in the current article, the operator's speed can vary at different parts of the path $p_j(\check{t})$, $j \in \mathcal{O}$, or even at the same segments of the path but at different times. However, we note that these time-varying speed profiles are imposed on the controller and are not subject to control.

1) Travel time penalty: Define the time spent by operator j traveling from node $p_{s,j}(\check{t})$ to $p_{s+1,j}(\check{t})$ at time $\check{t}$ taking the route with the index $r_{s,j}(\check{t})$ as

$$\mathcal{T}_{p_{s,j}(\check{t})\to p_{s+1,j}(\check{t})}^{r_{s,j}(\check{t})} = \frac{\mathcal{D}_{p_{s,j}(\check{t})\to p_{s+1,j}(\check{t})}^{r_{s,j}(\check{t})}}{v_{p_{s,j}(\check{t})\to p_{s+1,j}(\check{t})}^{r_{s,j}(\check{t})}(\check{t})}. \tag{9}$$

With $\mathcal{T}_{p_{s,j}(\check{t})\to p_{s+1,j}(\check{t})}^{r_{s,j}(\check{t})}$, the total time that an operator j spends traveling between locations is expressed as

$$J_{\mathrm{op},j}^{\mathrm{t}}(\check{t}) = \sum_{s=1}^{N_{\mathrm{s}}-1} \mathcal{T}_{p_{s,j}(\check{t})\to p_{s+1,j}(\check{t})}^{r_{s,j}(\check{t})}. \tag{10}$$

It is argued in [56] that long travel times (e.g., of professional drivers or commuters) may be associated with fatigue and deterioration of health, with physical inactivity mentioned as one of possible reasons. Therefore, minimizing (10) serves the purpose of reducing the operator's workload.

2) Waiting time penalty: Waiting times can be perceived by some operators as wasted time [57], generating discomfort. Hence, a second term is added in the cost function of the operator to consider his or her preferences regarding waiting and traveling:

$$
\begin{aligned}
J_{\mathrm{op},j}^{\mathrm{w}}(\breve{t}) = & \sum_{s=1}^{N_{\mathrm{s}}} \left(T_{s,j}^{\mathrm{act}}(\breve{t}) - T_{s,j}^{\mathrm{meas}}(\breve{t}) \right) \\
& + \sum_{s=1}^{N_{\mathrm{s}}-1} \left(T_{s+1,j}^{\mathrm{meas}}(\breve{t}) - T_{s,j}^{\mathrm{act}}(\breve{t}) - \frac{\mathcal{D}_{p_{s,j}(\breve{t}) \to p_{s+1,j}(\breve{t}),}^{r_{s,j}(\breve{t})}}{v_{s,j}^{\mathrm{op}}(\breve{t})} \right).
\end{aligned}
$$
(11)

The first part of $J_{\mathrm{op},j}^{\mathrm{w}}(\breve{t})$ accounts for the waiting time between taking measurements and applying a control action and the second part accounts for waiting time when traveling to a new location. To balance between $J_{\mathrm{op},j}^{\mathrm{t}}$ and $J_{\mathrm{op},j}^{\mathrm{w}}$ for each operator, the operators choose whether they prefer to travel or wait. Based on that, two mutually exclusive sets $\mathcal{O}_{\mathrm{wait}}$ and $\mathcal{O}_{\mathrm{travel}}$ are defined such that $\mathcal{O} = \mathcal{O}_{\mathrm{wait}} \cup \mathcal{O}_{\mathrm{travel}}$. The set $\mathcal{O}_{\mathrm{wait}}$ contains the indices of the operators who dislike waiting more than traveling, and set $\mathcal{O}_{\mathrm{travel}}$ contains the indices of the operators who dislike traveling more than waiting. Sets $\mathcal{O}_{\mathrm{wait}}$ and $\mathcal{O}_{\mathrm{travel}}$ are used to specify contributions from various operator-centric cost components for each operator (see (15)), where penalty (10) is used for operators $j \in \mathcal{O}_{\mathrm{travel}}$ (so the waiting time is not penalized) and penalty (11) is used for operators $j \in \mathcal{O}_{\mathrm{wait}}$ (therefore travel time is not penalized).

3) Operator's stress penalty: A third component of the operator cost function is motivated by understanding that different routes may have different levels of stress associated with them for different people. This may originate from the different perception of driving on a busy highway versus a local road, where one may prefer the quiet local roads, or the opposite – the convenience of highways versus using smaller, local roads [58,59]. The controller selects the route $r_{\ell,j}(\breve{t})$ taking into account the burden for the operator given his or her preferences:

$$
J_{\mathrm{op},j}^{\mathrm{s}}(\breve{t}) = \sum_{s=1}^{N_{\mathrm{s}}-1} \mathcal{S}_{j,p_{s,j}(\breve{t}) \to p_{s+1,j}(\breve{t})}^{r_{s,j}(\breve{t})}(\breve{t}) \mathcal{T}_{p_{s,j}(\breve{t}) \to p_{s+1,j}(\breve{t})}^{r_{s,j}(\breve{t})}, \quad (12)
$$

where the stress level variable $\mathcal{S}_{j,p_{s,j}(\breve{t}) \to p_{s+1,j}(\breve{t})}^{r_{s,j}(\breve{t})}(\breve{t})$ is related to the stress level of the operator j on a path segment between node $p_{s,j}(\breve{t})$ and $p_{s+1,j}(\breve{t})$ taking route $r_{s,j}(\breve{t})$. It is time-varying to allow one to assign different levels at different times in response to, e.g., traffic congestion or weather conditions. We allow here for the stress levels to differ amongst various operators. As seen in (12), to compute the overall stress level on a particular path segment $s = 1, \ldots, N_{\mathrm{s}}-1$ the stress level is multiplied by the time spent on that path segment.

4) Operator's energy level: Another aspect that the controller accounts for is tracking the operators' energy levels and scheduling their breaks. We define e_j to denote the energy level of the operator $j \in \mathcal{O}$. It is assumed that as operators travel, perform activities at scheduled locations, or wait in between other activities, the energy level drains linearly, possibly at a different rate for different operators. To express this, we use $\dot{e}_j = \Delta e_j^{\mathrm{activity}}$ with

$$
\Delta e_j^{\mathrm{activity}} = \begin{cases} \Delta e_j^{\mathrm{travel}} & \text{if operator } j \text{ travels,} \\ \Delta e_j^{\mathrm{waiting}} & \text{if operator } j \text{ waits,} \\ \Delta e_j^{\mathrm{act,meas}} & \text{if operator } j \text{ is at a location,} \\ & \quad \text{for measurements and actuation,} \\ \Delta e_j^{\mathrm{rest}} & \text{if operator } j \text{ takes a break,} \end{cases}
$$
(13)

where $\Delta e_j^{\mathrm{travel}} \leq 0$, $\Delta e_j^{\mathrm{waiting}} \leq 0$, $\Delta e_j^{\mathrm{act,meas}} \leq 0$, and $\Delta e_j^{\mathrm{rest}} \geq 0$. The energy level e_j cannot fall below a threshold e_j^{min}. To ensure this, the controller is free to schedule up to N_{rest} breaks for each operator. This is done with the help of a variable $T_j^{\mathrm{rest}}(\breve{t}) = (T_{1,j}^{\mathrm{rest}}(\breve{t}), \ldots, T_{N_{\mathrm{rest}},j}^{\mathrm{rest}}(\breve{t}))$, $T_{\ell,j}^{\mathrm{rest}}(\breve{t}) \in \mathbb{R}$, which denotes the times when the breaks for the operator j are to start, and a variable $\Delta T_j^{\mathrm{rest}}(\breve{t}) = (\Delta T_{1,j}^{\mathrm{rest}}(\breve{t}), \ldots, \Delta T_{N_{\mathrm{rest}},j}^{\mathrm{rest}}(\breve{t}))$, $\Delta T_{\ell,j}^{\mathrm{rest}}(\breve{t}) \geq 0$, which denotes the duration of the breaks of the operator j. Note that the controller may decide to schedule breaks at times when the energy level e_j is still relatively large, but it is worthwhile for the system to have a pause between various activities, when the operator would otherwise have to wait. We recognize that from the human well-being perspective, it may be sensible to impose a minimum duration of a break, but this is not considered in the current formulation of the controller.

5) Uniform workload penalty: Lastly, with multiple operators involved, we propose a penalty term J_{uni}, whose aim is to promote schedules with uniform workload between operators. The workload is expressed in terms of the average travel time $T_{\mathrm{tr},j}(\breve{t})$ given in (10) and the waiting time $T_{\mathrm{wait},j}(\breve{t})$ given in (11). We define the total time variable for operator j as $T_{\mathrm{tot},j}(\breve{t}) = T_{\mathrm{tr},j}(\breve{t}) + T_{\mathrm{wait},j}(\breve{t})$, with an average amongst all operators denoted as $T_{\mathrm{tot}}^{\mathrm{ave}}(\breve{t}) = \frac{1}{N_{\mathrm{op}}} \sum_{j \in \mathcal{O}} T_{\mathrm{tot},j}(\breve{t})$. Recall that when operators perform activities on network nodes, they are neither traveling nor waiting, so time is not accounted for in $T_{\mathrm{tot},j}(\breve{t})$. The penalty that we propose is

$$
J_{\mathrm{uni}}(\breve{t}) = \sum_{j \in \mathcal{O}} \left(T_{\mathrm{tot},j}(\breve{t}) - T_{\mathrm{tot}}^{\mathrm{ave}}(\breve{t}) \right)^2. \quad (14)
$$

Because the total time variable is considered in (14) as opposed to its individual components $T_{\mathrm{tr},j}$ and $T_{\mathrm{wait},j}$, the operators' preferences to spend more time traveling or waiting are not conflicting with this penalty (cf. (15)). Understandably, the choice of penalty (14) to incentivize the controller to spread the workload evenly amongst the operators could be different. For instance, one might also use the operators' energy levels.

6) The overall penalty: The cost function that describes the burden on the operators is a weighted sum of the objectives:

$$
\begin{aligned}
J_{\mathrm{op}}(\breve{t}) = & \sum_{j \in \mathcal{O}} \left(\alpha_{\mathrm{op},j}^{\mathrm{t}} J_{\mathrm{op},j}^{\mathrm{t}}(\breve{t}) + \alpha_{\mathrm{op},j}^{\mathrm{w}} J_{\mathrm{op},j}^{\mathrm{w}}(\breve{t}) + \alpha_{\mathrm{op},j}^{\mathrm{s}} J_{\mathrm{op},j}^{\mathrm{s}}(\breve{t}) \right) \\
& + \alpha_{\mathrm{uni}} J_{\mathrm{uni}}(\breve{t}),
\end{aligned}
$$
(15)

with weighting parameters $\alpha_{\mathrm{op},j}^{\mathrm{t}}, \alpha_{\mathrm{op},j}^{\mathrm{w}}, \alpha_{\mathrm{op},j}^{\mathrm{s}}, t = 1, \ldots, N_{\mathrm{op}}$, and α_{uni}. Observe that due to the definition and role of sets $\mathcal{O}_{\mathrm{wait}}$ and $\mathcal{O}_{\mathrm{travel}}$, we have $\alpha_{\mathrm{op},j}^{\mathrm{t}} = 0$ if $j \in \mathcal{O}_{\mathrm{wait}}$ and $\alpha_{\mathrm{op},j}^{\mathrm{w}} = 0$ if $j \in \mathcal{O}_{\mathrm{travel}}$.

D. Fuel consumption minimization

The fuel consumption cost can be formulated as

$$J_{\mathrm{f}}(\check{t}) = \sum_{j \in \mathcal{O}} \sum_{s=1}^{N_{\mathrm{s}}-1} \mathcal{R}(v_{p_{s,j}(\check{t}) \to p_{s+1,j}(\check{t})}^{r_{s,j}(\check{t})}) \mathcal{D}_{p_{s,j}(\check{t}) \to p_{s+1,j}(\check{t})}^{r_{s,j}(\check{t})}, \tag{16}$$

where $\mathcal{R}()$ is the rate of fuel consumption (in liters per distance unit) that depends on speed $v_{p_{s,j}(\check{t}) \to p_{s+1,j}(\check{t})}^{r_{s,j}(\check{t})}$. The exact form of the function $\mathcal{R}()$ is vehicle-specific, but generally resembles a quadratic function with a flat area of minimum value in the region of the highest fuel efficiency [60].

E. The new control algorithm

The optimal control problem to be solved whenever the operator provides new measurements is then

$$\min_{\substack{\mathscr{U}_j(\check{t}) \\ j \in \mathcal{O}}} w_0 J_{\mathrm{MoMPC}}(\check{t}) + w_1 J_{\mathrm{loc}}(\check{t}) + w_2 J_{\mathrm{op}}(\check{t}) + w_3 J_{\mathrm{f}}(\check{t}), \tag{17}$$

subject to

$$\hat{x}(\tau|\check{t}) \in \mathcal{X}, \ \forall \tau \in [\check{t}, \check{t}+T_{\mathrm{p}}], \tag{18}$$

$$u(T_{\ell,j}^{\mathrm{act}}|\check{t}) \in \mathcal{U}, \text{for } \ell = 1, \dots, N_{\mathrm{s}}, \ j \in \mathcal{O}, \tag{19}$$

$$T_{\ell+1,j}^{\mathrm{meas}} \geq T_{\ell,j}^{\mathrm{act}} + \mathcal{T}_{p_{\ell,j} \to p_{\ell+1,j}}^{r_{\ell,j}} + \Delta T_{\mathrm{d},p_{\ell+1,j}}^{\mathrm{arr}} + \Delta T_{\mathrm{d},p_{\ell,j}}^{\mathrm{dep}}, \tag{20}$$

$$\text{for } \ell = 1, \dots, N_{\mathrm{s}}-1 \text{ if } p_{\ell,j} \neq p_{\ell+1,j}, \ j \in \mathcal{O},$$

$$T_{\ell+1,j}^{\mathrm{meas}} \geq T_{\ell,j}^{\mathrm{act}} + \Delta T_{\mathrm{d},p_{\ell,j}}^{\mathrm{min}}, \tag{21}$$

$$\text{for } \ell = 1, \dots, N_{\mathrm{s}}-1 \text{ if } p_{\ell,j} = p_{\ell+1,j}, \ j \in \mathcal{O},$$

$$T_{\ell,j}^{\mathrm{act}} \geq T_{\ell,j}^{\mathrm{meas}} + \Delta T_{\mathrm{d},p_{\ell,j}}^{\mathrm{act}}, \text{ for } \ell = 1, \dots, N_{\mathrm{s}}, \ j \in \mathcal{O}, \tag{22}$$

$$T_1^{\mathrm{meas}} = \check{t}, \ p_{1,j} = v_{\mathrm{current},j}, \text{ for } j \in \check{\mathcal{O}}, \tag{23}$$

$$T_{1,j}^{\mathrm{meas}} \geq \check{t} + T_{\mathrm{busy},j} + \mathcal{T}_{\mathrm{loc}_j \to p_{1,j}(\check{t})}^{r_{1,j}} \tag{24}$$

$$p_{1,j} \in \mathcal{V}, \text{ for } j \notin \check{\mathcal{O}} \text{ and } \mathrm{st}_j = 0,$$

$$T_{1,j}^{\mathrm{meas}} \geq \check{t} + \mathcal{T}_{\mathrm{loc}_j \to p_{1,j}(\check{t})}^{r_{1,j}} \tag{25}$$

$$p_{1,j} = p_{1,j}(\check{t}_{\mathrm{prev}}), \text{ for } j \notin \check{\mathcal{O}} \text{ and } \mathrm{st}_j = 1,$$

$$T_{2,j}^{\mathrm{meas}} \leq \check{t} + T_{\mathrm{max}}, \ j \in \mathcal{O} \tag{26}$$

$$T_{1,j}^{\mathrm{rest}} \geq \check{t}, \tag{27}$$

$$T_{\ell+1,j}^{\mathrm{rest}} \geq T_{\ell,j}^{\mathrm{rest}}, \quad \text{for } \ell = 1, \dots, N_{\mathrm{rest}}-1, \ j \in \mathcal{O},$$

$$\Delta T_{\ell,j}^{\mathrm{rest}} \geq 0, \quad \text{for } \ell = 1, \dots, N_{\mathrm{rest}}, \ j \in \mathcal{O},$$

$$e_j \geq e_j^{\mathrm{min}} \tag{28}$$

$$\text{and } (2), (3), (5), (7), \tag{29}$$

where the time dependence $(\check{t})$ is omitted in the constraints for brevity, loc_j is the location of a traveling operator j at time $\check{t}$, $\mathscr{U}_j(\check{t}) = (p_j(\check{t}), r(\check{t}), T_j^{\mathrm{meas}}(\check{t}), T_j^{\mathrm{act}}(\check{t}), u_j^{\mathrm{op}}(\check{t}), T_j^{\mathrm{rest}}(\check{t}), \Delta T_j^{\mathrm{rest}}(\check{t}))$, and w_0, w_1, w_2, w_3 are positive weighting parameters. If the next location is different from the preceding one $(p_{\ell,j}(\check{t}) \neq p_{\ell+1,j}(\check{t}))$, the controller can freely schedule the corresponding measurement time instants $T_j^{\mathrm{meas}}(\check{t})$ and the actuation time instants $T_j^{\mathrm{act}}(\check{t})$. However, they must comply with the resulting sums of travel times between locations, the

times $T_{\mathrm{d},v_i}^{\mathrm{arr}}$ needed after arrival at a location $v_i \in \mathcal{V}$ to set up everything needed at that location, and the times $T_{\mathrm{d},v_i}^{\mathrm{dep}}$ needed at location v_i to finish the required work before being able to proceed to the next location; see (20). On the contrary, if the operator is scheduled to stay at the same location at some time $(p_{\ell,j}(\check{t}) = p_{\ell+1,j}(\check{t}))$, the actuation activity can only occur after a given minimal time delay $T_{\mathrm{d},p_{\ell,j}(\check{t})}^{\mathrm{min}}$, see (21). Constraint (22) represents the time delay that the operator needs to get ready to apply a control action after exchanging information with the controller, constraints (23)–(25) specify when the first measurement needs to be scheduled depending on whether the operator is traveling or is at a location, constraint (26) means that at least one additional location has to be scheduled for each operator within a given maximal idle time $T_{\mathrm{max}} \leq T_{\mathrm{p}}$ to provide the controller with new measurements from the system, constraint (27) relates to scheduling breaks, and constraint (28) introduces minimum operators' energy levels. Finally, constraint (31) defines the internal model used by the controller in its calculations of the predicted water levels and elapsed times.

The optimization problem (17)–(29) is a mixed-integer nonlinear programming problem. Various algorithms can be used to deal with such problems, e.g. genetic algorithms [61], or branch and bound [62].

To reformulate the algorithm in a distributed way to improve its scalability, the principles of the problem of multiple traveling salesmen could be used [53]. Alternatively, approximation methods for large-scale MINLP problems [63] can be used to obtain computationally lighter problem formulations. However, the human-related aspects and the sampling and asynchronous nature of the measurements and actuations make this a nontrivial task.

Finally, Table I summarizes the main elements of the proposed strategy. While there is no general rule for tuning the controller, it is always convenient to normalize the weight of each term in the cost, e.g., by choosing an initial value for each weighting parameter that makes the contribution of the corresponding term become one for average values of the corresponding variable. After the initialization, parameters can be adjusted to provide more or less relevance to each term according to the designer's goals.

IV. CASE STUDY

We use a numerical model of an irrigation canal in Dez in Iran [64, 65] to extend the preliminary version of TIO-MoMPC of [32] and compare its performance with that of the original MoMPC [17, 31]. This canal consists of 13 pools, see Figure 1, between which there are gates that the operator can raise or lower to allow more or less flow to the subsequent pool. For simplicity, we use flow rates through the gates as control inputs; however, gate positions can also be used. At the canal inlet, there is a head gate providing water from a reservoir created by a dam on the Dez River. We assume that the access to the head gate is not limited, and so measurements and actuations of the head gate are available at all times. In contrast, the remaining gates are serviced by a human operator, and so measurements can only be taken and a control action can only be applied when the operator is in a specific location.

Table I
MAIN ELEMENTS OF THE PROPOSED STRATEGY.

Cost function			
Eq.	Meaning	Symbol	Related to
(17)	Performance index optimized by the proposed controller, which comprises costs regarding overall system performance, the refreshment of measures on each location, the operators' well being, and fuel consumption.	w_0	System performance (6)
		w_1	Frequency of revisiting locations (8)
		w_2	Operators' welfare (15)
		w_3	Fuel consumption (16)
(6)	Quadratic cost of the overall system calculated at time $\check{t}$ along a horizon $\tau \in [\check{t}, \check{t} + T_{\mathrm{p}}]$.	Q	Predicted state evolution $\hat{x}^{\mathrm{T}}(\tau\|\check{t})$
		R	Optimized input trajectory $u(\tau\|\check{t})$
(8)	Cost that accumulates the time since the last measurement in each location.	$\alpha_{\mathrm{loc},i}$	Relevance of each spot $i \in [1, N]$
(15)	It comprises weighted costs dealing with issues that affect the welfare of operators, namely, travel and waiting times, stress and energy levels, and distribution of workload among operators.	$\alpha_{\mathrm{op},j}^{\mathrm{t}}$	Travel times (10)
		$\alpha_{\mathrm{op},j}^{\mathrm{w}}$	Waiting times (11)
		$\alpha_{\mathrm{op},j}^{\mathrm{s}}$	Stress levels (12)
		α_{uni}	Workload distribution (14)
(16)	Cost of the fuel consumed along route.	$\mathcal{R}()$	Fuel consumption function.
Constraints			
(18)	Constraints on states of the irrigation canal.	$\mathcal{X}$	Limits of water levels and flows.
(19)	Constraints on inputs of the irrigation canal	$\mathcal{U}$	Limits of gates and water flows
(20)	Constraints on the separation between consecutive measuring and actuation activities when the operator is traveling	$T_{\ell+1,j}^{\mathrm{meas}}$	The measurement time instant
		$T_{\ell,j}^{\mathrm{act}}$	The actuation time instant
		$\mathcal{T}_{p_{\ell,j} \to p_{\ell+1,j}}^{\ell,j}$	Travel time from ℓ to $\ell+1$
		$\Delta T_{\mathrm{d},p_{\ell+1,j}}^{\mathrm{arr}}$	Time needed after arrival
		$\Delta T_{\mathrm{d},p_{\ell,j}}^{\mathrm{dep}}$	Time needed before departure
(21)	Constraints on the separation between consecutive measuring and actuation activities when the operator is not traveling	$\Delta T_{\mathrm{d},p_{\ell,j}}^{\mathrm{min}}$	Time between act. and meas.
(24)	Constraints on scheduling the measuring time instant of the first location on a current route	$T_{\mathrm{busy},j}$	Time to finish at a current location
		$\mathcal{T}_{\mathrm{loc}_j \to p_{1,j}}^{1,j}(\check{t})$	Travel time to the first location
(26)	Constraints on scheduling of the second location	T_{max}	Maximum time of the sec. location
(27)	Constraints on scheduling the rest time	$T_{\ell,j}^{\mathrm{rest}}$	Resting time instant
		$\Delta T_{\ell,j}^{\mathrm{rest}}$	Minimal resting duration
(28)	Constraints on the operators' energy level	e_j	Operator energy level
		e_j^{min}	Minimal energy level

We approximate problem (17)–(29) using a discrete-time model with a sample and a control step of $T_{\mathrm{c}} = 5$ minutes to ease the implementation. However, this way of implementation implies that the time instants $T_j^{\mathrm{meas}}(\check{t})$ and $T_j^{\mathrm{act}}(\check{t})$ are no longer real-valued variables but instead they are integers (i.e. sample steps). The genetic algorithm (GA) with a random feasible initial population implemented in the Matlab Global Optimization Toolbox is used together with a quadratic programming (QP) solver from CPLEX to solve the optimization problem. GA involves a metaheuristic nonlinear optimization procedure that starts from a random population of *genes* representing possible solutions, which are iteratively mixed and mutated based on their performance to minimize the desired cost function, providing the best solution available after a certain condition is met (e.g., based on the maximum number of generations and execution time) [66, 67]. QP algorithms can find the optimal solution of a continuous quadratic function subject to linear constraints in polynomial time using well-known algorithms, e.g., interior-point methods [68, 69]. These two optimization methods are combined as follows: the solution at every activation is first found by the GA passing a candidate route to the QP solver which then determines the optimal flows through the gates on the route and passes them back to GA. These together are used to compute the cost function by the GA and at the end the optimal route and flows follow. The pseudocode of the implemented approach is shown in Algorithm 1.

Remark 3: As it is common in metaheuristic methods, there are no guarantees regarding the convergence of GA unless sufficient time is given to find the global optimum [70]. Otherwise, GA employs the best solution obtained in the available time. One way to guarantee that GA provides performance equal to or superior to that of MoMPC is to use the MoMPC solution as one of the initial seeds of the GA method. In this way, it fixes a lower bound on the performance of GA. Also, note that there are some well-known alternatives for reducing the computation burden, e.g., using surrogate models, approximating integer programming with continuous domain optimization, optimizing over a coarser grid, employing shrinking prediction horizons [71], etc.

To assess the performance of the proposed method, we compare the results obtained with those of the algorithm in [17, 31]. We use the process model identical to the prediction model, $N_{\mathrm{s}} = 8$, prediction horizon $N_{\mathrm{p}} = 48$, and control horizon $N_{\mathrm{c}} = 48$, where these last two parameters belong to the optimization problem used in [17, 31] and, respectively, correspond to the number of time steps included in the performance index and the number of instants for which the input is to be determined. To allow for a fair comparison, the model of the system is assumed known to the controller and some operational parameters that were not considered in the previous approach are set to 0, namely, the time to perform necessary tasks upon arrival to a new location ($\Delta T_{\mathrm{d},v}^{\mathrm{arr}}$), the time to implement the actuation ($\Delta T_{\mathrm{d},v}^{\mathrm{act}}$), and also the time

---

Algorithm 1: Pseudocode of the genetic algorithm

Data: N_{members}, N_{iter}

Create population of N_{members} random solutions of
  Problem (17) s.t. (18)–(29);

$l \leftarrow 1$;

while $l \leq N_{\text{iter}}$ **do**

  $l \leftarrow l + 1$;

  Rank members of the current population by
  $w_0 J_{\text{MoMPC}}(\check{t}) + w_1 J_{\text{loc}}(\check{t}) + w_2 J_{\text{op}}(\check{t}) + w_3 J_{\text{f}}(\check{t})$;

  Start the new population with the top 5% members;

  while *new population size* $\leq N_{\text{members}}$ **do**

    Select and rank a random subset of 4 members
     of current population;

    Generate new member for new population by
     mutating the subset's top member or
     randomly combining its two top members
     (satisfying (18)–(29));

  end

end

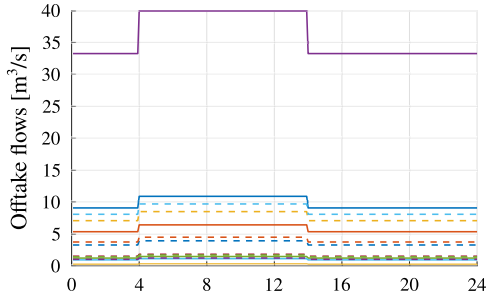Return solution with lowest cost;

Figure 3. Offtake profile used in the case study, which provides the hourly representation of the water taken from each section of the canal for farming activities. From the viewpoint of the internal model of the controller, this outflow is interpreted as an exogenous input.

needed before departing from a location ($\Delta T_{\text{d},v}^{\text{dep}}$). In addition, the length of the prediction horizon and the time step are considered to be the same, i.e., $T_{\max} = N_c T_c$, and $\Delta T_{\text{d},v}^{\min} = T_c$. A number of disturbance offtakes are employed, see Figure 3. We use $\alpha_{\text{loc},1} = \alpha_{\text{loc},2} = 10^{-6}$, $\alpha_{\text{op},1}^{\text{w}} = 10^{-3}$, $\alpha_{\text{op},2}^{\text{w}} = 0$, $\alpha_{\text{op},1}^{\text{t}} = 0$, $\alpha_{\text{op},2}^{\text{t}} = 10^{-3}$, $w_1 = 1$, $w_2 = 1$, $w_3 = 10^{-6}$. The operators' nominal velocity is 30 km/h, operator 1 starts at reach 1 at full energy charge and operator 2 starts at reach 13 at 80% energy. The energy is drained at 1% per sample step and the recharge rate is 15% per sample step.

We use the posterior performance index $J_{\text{oper.\,obj.}} = \sum_{k=1}^{N_{\text{f}}} \left(x^{\text{T}}(k) Q x(k) + u^{\text{T}}(k) R u(k) \right)$, which relates to how well the process is executed and thus the operational objectives are met, and $J_{\Delta \text{t}} = \sum_{i=2}^{13} \sum_{k=1}^{N_{\text{f}}} \Delta t_i(k)$, which relates to how often individual gates are visited. The parameter $N_{\text{f}} = 288$ (a period of 24 hours) denotes the total number of simulation steps. The weighting matrices are $Q = 100I$ and $R = 0.01I$.

Remark 4: The determination of weighting parameters remains an open issue. To improve the trial-and-error process followed in this article, one can normalize the components in the cost function and then increase the weight of more critical

elements based on the designer's preferences. Another possible alternative is to reformulate the problem as a multi-objective optimization problem and search for a Pareto optimal solution.

A. Long computation time set-up

The first set of simulations are set up to allow a considerable computation time to solve the optimization problem (17)–(29) at every activation. As the simulations are performed on a high-performance computer cluster consisting of machines of various computational power, to indirectly control how much computation time is used per activation step, we limit the number of generations per one genetic algorithm run. In the first case, the maximum number of generations is 500, and the population size is 5000. These result in computations taking on average per computation step 2462.4 s for the TIO-MoMPC method and 2440.0 s for the MoMPC method. Although these computation times are large, they are of the order of magnitude of the sampling times of large canals. As will be seen in the following subsections, it is straightforward to limit the computation burden by reducing the number of generations of the GA. Therefore, the optimizer can be adjusted to apply the best solution found within the available computation time.

To illustrate the benefits of scheduling the timing of measures and actions (rather than following strictly predetermined travel times between gates as in MoMPC [17, 31]), the cost function accounts only for the J_{MoMPC} component, thus measuring solely the performance of the process.

In this scenario, an operator is working along the canal. The posterior performance index is $J_{\text{oper.\,obj.}} = 261.65$ for the TIO-MoMPC method, and the corresponding water levels and flows in all pools as well as the path of the operator are shown in Figure 4 (upper-left plot). In turn, $J_{\text{oper.\,obj.}} = 339.75$ for MoMPC from [17, 31], see Figure 4 (upper-right plot). Thus, the new method gives a 23% improvement. At the same time, while not directly used in the optimized cost function of either method in the case study, we observe that $J_{\Delta \text{t}} = 3.41 \cdot 10^7$ for the TIO-MoMPC method and $J_{\Delta \text{t}} = 3.05 \cdot 10^7$ for MoMPC. Such results are expected: better control performance is achieved in terms of the $J_{\text{oper.\,obj.}}$ index but, since there are waiting periods allowed, overall the frequency of visits to all gates is decreased, and, simultaneously, there are longer periods of time between the operator's visit to each gate. In the simulation, this did not cause any problems due to the absence of model-plant mismatch and model uncertainty. However, in reality, when the prediction model never truly matches the real system and there are uncertain terms in the model, the canal reaches need to be monitored regularly to correct any potential model-system discrepancies. Therefore, the use of the network monitoring penalty (8) is key in real applications, and is indeed included in the cost function used in the next subsection.

B. Tractable controller set-up

In the second set of simulations, the maximum computation time allowed per sample step is reduced by forcing the GA solver to return a solution after 15 generations with the population size of 5000. Average computation times per control step are reported below. We look at four scenarios:
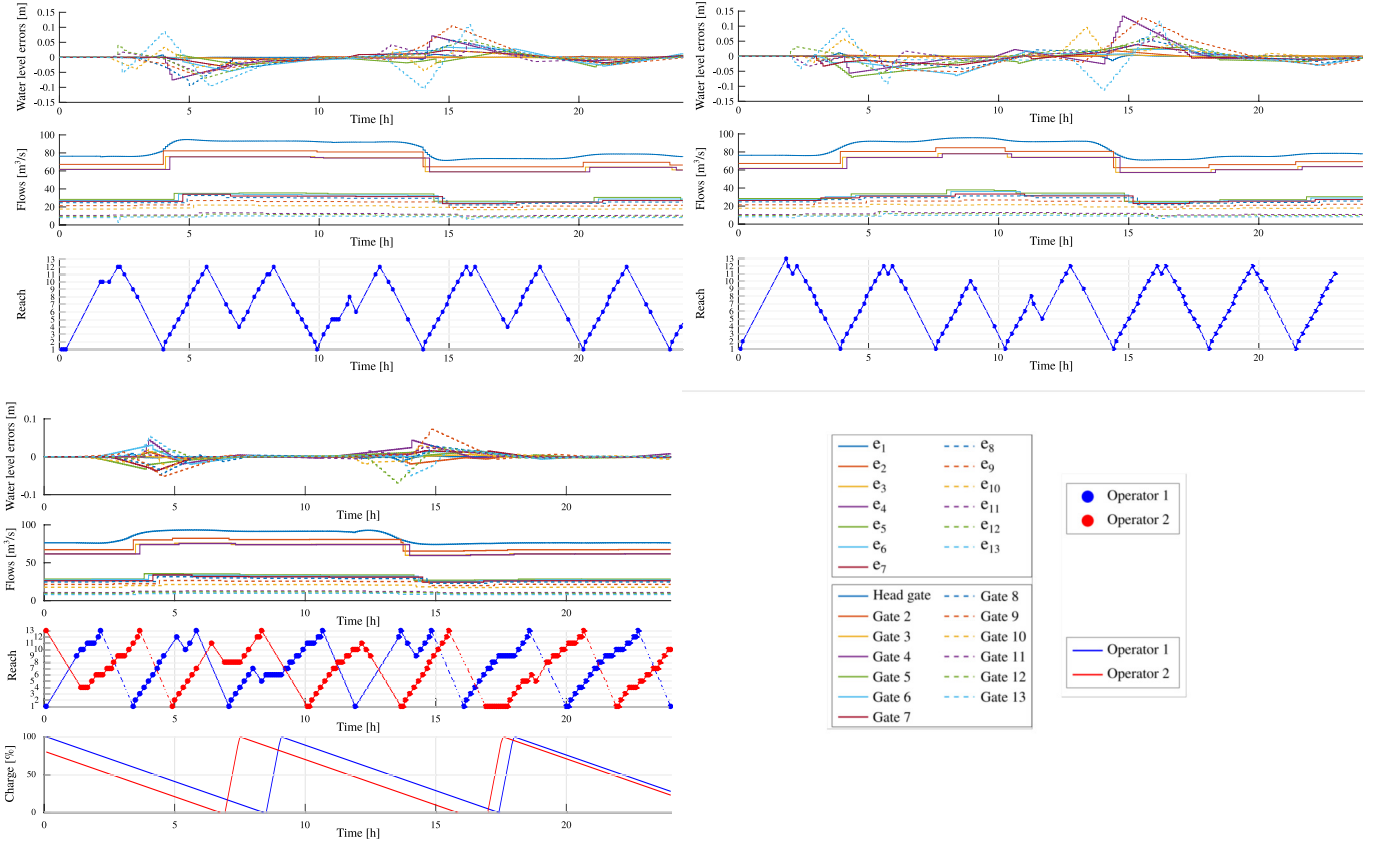
Figure 4. Upper plots: Simulation results for the TIO-MoMPC (left) and MoMPC (right) methods. Lower plots: The median simulation results for Scenario A (left) and legend for all plots (right). Within each plot, results are presented in the following order (top to bottom) water levels in the pools, flows in the pools, and path of the operator.

Table II
MEAN POSTERIOR RESULTS FOR SCENARIOS A, B, C, AND D.

	A	B	C	D
$J_{\mathrm{oper.\,obj.}}$	106.3	102.1	569.1	494.5
$J_{\Delta\mathrm{t}}$	$1.53 \cdot 10^7$	$1.59 \cdot 10^7$	$3.25 \cdot 10^7$	$3.25 \cdot 10^7$

A) TIO-MoMPC with two operators and two routes for some nodes (average computation time is 111.1 s)

B) TIO-MoMPC with two operators and one route (average computation time is 111.1 s)

C) TIO-MoMPC with one operator and one route (average computation time is 104.4 s)

D) MoMPC with one operator and one route (average computation time is 104.1 s)

Due to the early termination of the optimization routine at every control step and the stochastic nature of the genetic algorithm, the simulations are run multiple times with the same initial conditions. Then, the results are collectively analyzed in terms of their statistical significance, see Figure 5. The resulting mean values across the populations for the four scenarios, respectively, are given in Table II.

We use the two-sample Welch's test [72] to compare the results for the four scenarios. It can be shown using the Jarque-Bera test [73], that the data are consistent with the normality assumption. In addition, we note that the two-sample Welch's
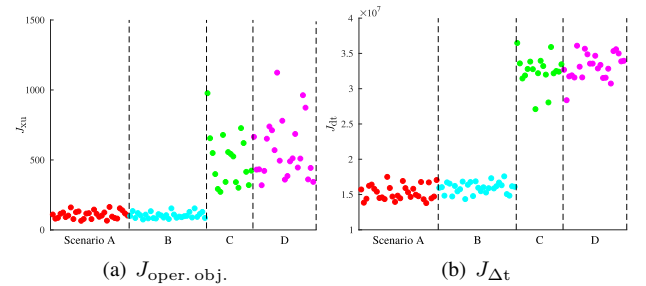

(a) $J_{\mathrm{oper.\,obj.}}$ (b) $J_{\Delta\mathrm{t}}$

Figure 5. The obtained values of $J_{\mathrm{oper.\,obj.}}$ and $J_{\Delta\mathrm{t}}$ for the population of simulation runs for Scenarios A-D.

test is robust to small sample sizes and non-normality of the distribution of the data.

We test the null hypothesis that the mean value of the posterior performance indices $J_{\mathrm{oper.\,obj.}}$ and $J_{\Delta\mathrm{t}}$ is higher for a particular scenario (A, B, C, and D) than for other scenarios.

Based on the probability values (p-values) reported in Table III and using the one-tailed significance level of 0.001, we accept the alternative hypotheses claiming that the mean performance indices $J_{\mathrm{oper.\,obj.}}$ and $J_{\Delta\mathrm{t}}$ for scenarios A and B are lower than for scenarios C and D. The observed data do not show any significant differences in the mean performance index $J_{\mathrm{oper.\,obj.}}$ between scenarios A and B. At the same time, the data show weaker evidence (p-value of $0.35 \cdot 10^{-2}$) that the

Table III
P-VALUES TESTING THE NULL HYPOTHESIS OF INDICES $J_{\text{oper. obj.}}$ AND $J_{\Delta\text{t}}$ IN SCENARIOS A TO D (COLS.) EXCEEDING THEIR VALUES IN OTHER SCENARIOS (ROWS).

|		A	B	C	D
$J_{\text{oper. obj.}}$	A	N/A	0.74	$4.48 \cdot 10^{-8}$	$7.95 \cdot 10^{-11}$
	B	0.26	N/A	$3.98 \cdot 10^{-8}$	$7.13 \cdot 10^{-11}$
	C	1	1	N/A	0.12
	D	1	1	0.88	N/A
$J_{\Delta\text{t}}$	A	N/A	$0.35 \cdot 10^{-2}$	$1.41 \cdot 10^{-19}$	$1.52 \cdot 10^{-31}$
	B	1	N/A	$2.90 \cdot 10^{-18}$	$1.46 \cdot 10^{-28}$
	C	1	1	N/A	0.17
	D	1	1	0.83	N/A

Figure 6. The fixed travel time of the original route between pools 5 and 13 (dashed line), and the time-of-day dependent travel time of the new route (solid line).

mean performance index $J_{\Delta\text{t}}$ for scenario A is lower than for scenario B. This indicates that by introducing additional faster routes, the actuation and measurement frequency of the system increases. There are no statistically significant differences in the mean performance indices $J_{\text{oper. obj.}}$ and $J_{\Delta\text{t}}$ between scenarios C and D.

Evidently, the multiple-route algorithm is able to handle the multiple route formulation tracking the operator energy levels and scheduling adequate breaks for the operators. This all is achieved while controlling the system's process performance and thus converging to the desired setpoints. For completeness, the graph showing the median simulation results for Scenario A is given in Figure 4 (lower-left plot) while the plots for Scenarios B-D are omitted due to space limitations.

Finally, note that the case with two routes is created by artificially adding extra links between some pools in the Dez canal network (which originally only had a single route between any two sets of pools). The properties of these routes vary throughout the day, with an increased travel time around the morning (8am) and afternoon (5pm) peak times; see Figure 6. This way, taking the 'highway' routes is faster off-peak but slower at peak times. Note that to simplify the algorithm implementation and the analysis of the results, we do not consider the operators' preferences related to what kind of roads they like traveling on, as described with the help of the stress levels $\mathcal{S}$ (cf. (12)).

C. Discussion

We have considered a practical application where the operational objective is to regulate water levels of a realistic irrigation canal model while considering operators' well-being. In this regard, there is a trade-off between performance and computational requirements, which are strongly influenced by the number of iterations employed by the GA method. Since usual sampling times in these applications are of the order of minutes, this issue is not critical and, as can be seen in Figure 4, average errors in water level regulation are close to zero in all cases, with peaks below 15 cm, which is excellent performance considering that the canal is manually operated.
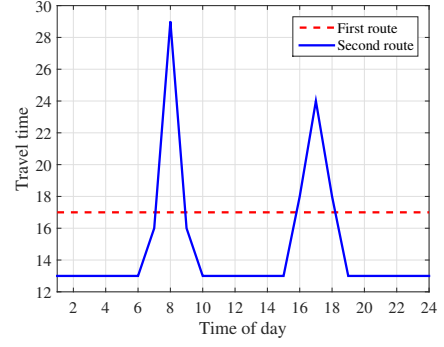
The results show that when the computation resources are limited, a global minimum is not achieved due to the early termination of the solver. However, the TIO-MoMPC still achieves a performance comparable to that of the MoMPC of [17, 31] for the original regulation objectives using an identical simulation setup, and outperforms this controller for the newly introduced goals (e.g., the consideration of the well-being of the operators, their energy levels and preferences for either waiting or traveling). On the other hand, the TIO-MoMPC method clearly outperforms MoMPC when given more computation resources because it has a larger search space, although it requires more time to find a high-quality result. In Section IV.B, allowing the GA more time per control step yields much better performance than the other method, but global convergence is untested. Therefore, the two sets of simulations (Sections IV.B and C) suggest a trade-off between computation requirements and performance.

Finally, it is worth noting that the current case study considers only one operator. However, we propose a generic multi-operator problem that enables the schedules for all operators to be recomputed on demand. This approach is particularly useful in cases where multiple operators are involved, or when dealing with extreme events that require continuous and careful replanning of measurements and actions by the operators. Likewise, each particular application needs to assess the minimal number of human operators required to satisfy the observational demand while accounting for factors such as staff stress and workload to ensure that errors do not accumulate to an intolerable level.

V. CONCLUSIONS

A human-in-the-loop control problem for a network system has been considered. Human operators are considered as moving sensors and actuators providing a central controller with measurements from visited locations and performing control actions requested by the controller. Given the limited sensing and actuating actions of the operators, the precise timings of their measuring and actuating actions have been used as optimization variables in a time instant optimization MPC framework to improve performance with respect to the method previously introduced in the literature.

The simulation results demonstrate that the new method is able to improve the operational performance, but more computation resources are needed. Also, the new method uses a multi-criteria objective function to explicitly balance: i) the evolution of the system and the routes followed by operators; ii) network monitoring; iii) the operators' burden (including travel and waiting times, stress and energy levels, and workload); and iv) fuel consumption. The original MoMPC approach was mainly focused on the first of the elements mentioned, and its rationale is clear in the context of an irrigation canal management problem. The same holds for the fuel consumption cost, which is also easy to implement. The network monitoring cost represents a practical approach to limit the uncertainty in the evolution of the system outputs that must be monitored by the operators and is consistent with the type of application considered. The most original contribution of this work lies in the operator-centric costs, which stem from issues that appear in the references given along the article, many of them coming from the field of psychology. Certainly, we do not claim that the list of elements considered is exhaustive, but we believe that this article contributes to the design of controllers that are operator-aware for human-in-the-loop processes. Similarly, the assessment performed shows some of the trade-offs that occur when these aspects are integrated. Therefore, the expansion of this line of work requires joint efforts from other fields such as psychology. In this regard, the versatility of the MPC framework will be beneficial for the inclusion of other aspects related to the operator.

We also acknowledge some limitations of our work that require further research. In particular, observability issues have been greatly simplified by considering that an estimate of the state is available to the controller. Although it is clear that systems currently controlled by humans must have features that allow for this type of operation, our contribution can help increase performance with minimal investment, there can be a complex interplay between the route followed by the operator and fundamental properties such as controllability and observability that is worth exploring.

Future work includes identifying more precise models of human behavior for the model predictive controller. The problem of observer design for the settings considered will also be explored. Moreover, we will work towards solving the problem using a distributed control approach.

REFERENCES

[1] G. Conde, N. Quijano, and C. Ocampo-Martinez, "Modeling and control in open-channel irrigation systems: A review," *Annual Reviews in Control*, vol. 51, pp. 153–171, 2021.

[2] M. Lewis, H. Wang, P. Velagapudi, P. Scerri, and K. Sycara, "Using humans as sensors in robotic search," in *Proceedings of the 12th International Conference on Information Fusion*, Seattle, WA, July 2009, pp. 1249–1256.

[3] T. Kaupp, A. Makarenko, S. Kumar, B. Upcroft, and S. Williams, "Operators as information sources in sensor networks," in *Proceedings of the 2005 IEEE/RSJ International Conference on Intelligent Robots and Systems*, Alberta, Canada, Aug 2005, pp. 936–941.

[4] J. M. Maestre, "Human in the loop model predictive control methods for water systems," *Systems, Control and Information*, vol. 65, no. 9, pp. 352–357, 2021.

[5] M. Inoue and V. Gupta, ""weak" control for human-in-the-loop systems," *IEEE Control Systems Letters*, vol. 3, no. 2, pp. 440–445, 2019.

[6] M. I. Fernández, P. Chanfreut, I. Jurado, and J. M. Maestre, "A data-based model predictive decision support system for inventory management in hospitals," *IEEE Journal of Biomedical and Health Informatics*, vol. 25, no. 6, pp. 2227–2236, 2021.

[7] H.-N. Wu, X.-M. Zhang, and R.-G. Li, "Synthesis with guaranteed cost and less human intervention for human-in-the-loop control systems," *IEEE Transactions on Cybernetics*, vol. 52, no. 8, pp. 7541–7551, 2022.

[8] Z. Chen, B. B. Park, and J. Hu, "Design and evaluation of a human-in-the-loop connected cruise control," *IEEE Transactions on Vehicular Technology*, vol. 71, no. 8, pp. 8104–8115, 2022.

[9] A. Perrusquía and W. Yu, "Human-in-the-loop control using euler angles," *J. Intell. Robotic Syst.*, vol. 97, no. 2, pp. 271–285, 2020.

[10] S. Musić and S. Hirche, "Passive noninteracting control for human-robot team interaction," in *2018 IEEE Conference on Decision and Control (CDC)*, 2018, pp. 421–427.

[11] M. W. S. Atman, T. Hatanaka, Z. Qu, N. Chopra, J. Yamauchi, and M. Fujita, "Motion synchronization for semi-autonomous robotic swarm with a passivity-short human operator," *International Journal of Intelligent Robotics and Applications*, vol. 2, no. 2, pp. 235–251, 2018.

[12] Y. Ding, M. Kim, S. Kuindersma, and C. J. Walsh, "Human-in-the-loop optimization of hip assistance with a soft exosuit during walking," *Science Robotics*, vol. 3, no. 15, 2018.

[13] M. Menner, L. Neuner, L. Lünenburger, and M. N. Zeilinger, "Using human ratings for feedback control: A supervised learning approach with application to rehabilitation robotics," *IEEE Transactions on Robotics*, vol. 36, no. 3, pp. 789–801, 2020.

[14] H. Su, W. Qi, C. Yang, J. Sandoval, G. Ferrigno, and E. De Momi, "Deep neural network approach in robot tool dynamics identification for bilateral teleoperation," *IEEE Robotics and Automation Letters*, vol. 5, no. 2, pp. 2943–2949, 2020.

[15] M. Ma, W. Lin, D. Pan, Y. Lin, P. Wang, Y. Zhou, and X. Liang, "Data and decision intelligence for human-in-the-loop cyber-physical systems: Reference model, recent progresses and challenges," *Journal of Signal Processing Systems*, vol. 90, no. 8, pp. 1167–1178, 2018.

[16] R. Schlossman, M. Kim, U. Topcu, and L. Sentis, "Toward achieving formal guarantees for human-aware controllers in human-robot interactions," in *2019 IEEE/RSJ International Conference on Intelligent Robots and Systems (IROS)*, 2019, pp. 7770–7776.

[17] P. J. van Overloop, J. M. Maestre, A. D. Sadowska, E. F. Camacho, and B. De Schutter, "Human-in-the-loop model predictive control of an irrigation canal [applications of control]," *IEEE Control Systems Magazine*, vol. 35, no. 4, pp. 19–29, 2015.

[18] K. Hara, M. Inoue, and J. M. Maestre, "Data-driven human modeling: Quantifying personal tendency toward laziness," *IEEE Control Systems Letters*, vol. 5, no. 4, pp. 1219–1224, 2020.

[19] H. Wu and X. Zhang, "Stochastic stability analysis and synthesis of a class of human-in-the-loop control systems," *IEEE Transactions on Systems, Man, and Cybernetics: Systems*, pp. 1–11, 2020.

[20] S. Hirche and M. Buss, "Human-oriented control for haptic teleoperation," *Proceedings of the IEEE*, vol. 100, no. 3, pp. 623–647, March 2012.

[21] W. Zeiler, D. Vissers, R. Maaijen, and G. Boxem, "Occupants' behavioural impact on energy consumption: 'human-in-the-loop' comfort process control," *Architectural Engineering and Design Management*, vol. 10, no. 1-2, pp. 108–130, 2014.

[22] X. Hu and G. Lodewijks, "Detecting fatigue in car drivers and aircraft pilots by using non-invasive measures: The value of differentiation of sleepiness and mental fatigue," *Journal of Safety Research*, vol. 72, pp. 173–187, 2020.

[23] K. C. Gross, K. Baclawski, E. S. Chan, D. Gawlick, A. Ghoneimy, and Z. H. Liu, "A supervisory control loop with prognostics for human-in-the-loop decision support and control applications," in *2017 IEEE conference on cognitive and computational aspects of situation management (CogSIMA)*. IEEE, 2017, pp. 1–7.

[24] S. A. S. Mousavi, F. Matveeva, X. Zhang, T. M. Seigler, and J. B. Hoagg, "The impact of command-following task on human-in-the-loop control behavior," *IEEE Transactions on Cybernetics*, pp. 1–15, 2020.

[25] M. Nagahara, D. E. Quevedo, and D. Nešić, "Maximum hands-off control: a paradigm of control effort minimization," *IEEE Transactions on Automatic Control*, vol. 61, no. 3, pp. 735–747, 2015.

[26] T. Hatanaka, N. Chopra, J. Yamauchi, and M. Fujita, "A passivity-based approach to human–swarm collaboration and passivity analysis of human operators," *Trends in Control and Decision-Making for Human–Robot Collaboration Systems*, pp. 325–355, 2017.

[27] M. Protte, R. Fahr, and D. E. Quevedo, "Behavioral economics for human-in-the-loop control systems design: Overconfidence and the hot hand fallacy," *IEEE Control Systems Magazine*, vol. 40, no. 6, pp. 57–76, 2020.

[28] D. Sidoti, G. V. Avvari, M. Mishra, L. Zhang, B. K. Nadella, J. E. Peak, J. A. Hansen, and K. R. Pattipati, "A multiobjective path-planning algorithm with time windows for asset routing in a dynamic weather-impacted environment," *IEEE Transactions on Systems, Man, and Cybernetics: Systems*, vol. 47, no. 12, pp. 3256–3271, Dec 2017.

[29] C. Chang, G. Yu, T. Wang, and C. Lin, "Path construction and visit scheduling for targets by using data mules," *IEEE Transactions on Systems, Man, and Cybernetics: Systems*, vol. 44, no. 10, pp. 1289–1300, Oct 2014.

[30] C. Murray and W. Park, "Incorporating human factor considerations in unmanned aerial vehicle routing," *IEEE Transactions on Systems, Man, and Cybernetics: Systems*, vol. 43, no. 4, pp. 860–874, July 2013.

[31] J. M. Maestre, P. J. van Overloop, M. Hashemy, A. Sadowska, and E. Camacho, "Mobile model predictive control for irrigation canals," in *Proceedings of IEEE Conference on Decision and Control*, Los Angeles, CA, Dec. 2014, pp. 4881–4886.

[32] A. Sadowska, P. J. van Overloop, J. M. Maestre, and B. De Schutter, "Human-in-the-loop control of an irrigation canal using time instant optimization model predictive control," in *Proceedings of 2015 European Control Conference*, July 2015, pp. 3274–3279.

[33] B. De Schutter and B. De Moor, "Optimal traffic light control for a single intersection," *European Journal of Control*, vol. 4, no. 3, pp. 260–276, 1998.

[34] B. Dekens, A. Sadowska, P. J. van Overloop, D. Schwanenberg, and B. De Schutter, "Gradient-based hybrid model predictive control using time instant optimization for Dutch regional water systems," in *Proceedings of the 2014 European Control Conference*, Strasbourg, France, June 2014, pp. 1343–1348.

[35] C. Godsil and G. Royle, *Algebraic Graph Theory*. New York: Springer, 2001.

[36] D. Helbing, "Gas-kinetic derivation of Navier-Stokes-like traffic equations," *Physical Review E*, vol. 53, pp. 2366–2381, Mar 1996.

[37] G. Corriga, F. Patta, S. Sanna, and G. Usai, "A mathematical model for open-channel networks," *Applied Mathematical Modelling*, vol. 3, no. 1, pp. 51–54, 1979.

[38] J. Schuurmans, A. J. Clemmens, S. Dijkstra, A. Hof, and R. Brouwer, "Modeling of irrigation and drainage canals for controller design," *Journal of irrigation and drainage engineering*, vol. 125, no. 6, pp. 338–344, 1999.

[39] N. C. Jacob and R. Dhib, "Unscented Kalman filter based nonlinear model predictive control of a LDPE autoclave reactor," *Journal of Process Control*, vol. 21, no. 9, pp. 1332–1344, 2011.

[40] K. Myers and B. Tapley, "Adaptive sequential estimation with unknown noise statistics," *IEEE Transactions on Automatic Control*, vol. 21, no. 4, pp. 520–523, Aug. 1976.

[41] Zs. Lendek, T. Guerra, R. Babuška, and B. De Schutter, *Stability Analysis and Nonlinear Observer Design Using Takagi-Sugeno Fuzzy Models*, ser. Studies in Fuzziness and Soft Computing. Berlin, Germany: Springer, 2010, vol. 262.

[42] G. Goodwin, H. Haimovich, D. Quevedo, and J. Welsh, "A moving horizon approach to networked control system design," *IEEE Transactions on Automatic Control*, vol. 49, no. 9, pp. 1427–1445, Sept 2004.

[43] D. Lahat, T. Adali, and C. Jutten, "Multimodal data fusion: An overview of methods, challenges, and prospects," *Proceedings of the IEEE*, vol. 103, no. 9, pp. 1449–1477, Sept 2015.

[44] L. P. Rodriguez, J. M. Maestre, E. F. Camacho, and M. C. Sánchez, "Decentralized ellipsoidal state estimation for linear model predictive control of an irrigation canal," *Journal of Hydroinformatics*, vol. 22, no. 3, pp. 593–605, 2020.

[45] F. Küsters and S. Trenn, "Switch observability for switched linear systems," *Automatica*, vol. 87, pp. 121–127, 2018.

[46] A. Tanwani, H. Shim, and D. Liberzon, "Observability implies observer design for switched linear systems," in *Proceedings of the 14th international conference on Hybrid systems: computation and control*, 2011, pp. 3–12.

[47] A. Sadowska, B. De Schutter, and P.-J. van Overloop, "Delivery-oriented hierarchical predictive control of an irrigation canal: event-driven versus time-driven approaches," *IEEE Transactions on Control Systems Technology*, vol. 23, no. 5, pp. 1701–1716, 2015.

[48] P. Sopasakis, P. Patrinos, and H. Sarimveis, "MPC for sampled-data linear systems: Guaranteeing constraint satisfaction in continuous-time," *IEEE Transactions on Automatic Control*, vol. 59, no. 4, pp. 1088–1093, Apr. 2014.

[49] L. Magni and R. Scattolini, "Model predictive control of continuous-time nonlinear systems with piecewise constant control," *IEEE Transactions on Automatic Control*, vol. 49, no. 6, pp. 900–906, June 2004.

[50] M. B. Saltık, L. Özkan, J. H. A. Ludlage, S. Weiland, and P. M. J. Van den Hof, "An outlook on robust model predictive control algorithms: Reflections on performance and computational aspects," *Journal of Process Control*, vol. 61, pp. 77–102, 2018.

[51] J. M. Grosso, P. Velarde, C. Ocampo-Martinez, J. M. Maestre, and V. Puig, "Stochastic model predictive control approaches applied to drinking water networks," *Optimal Control Applications and Methods*, vol. 38, no. 4, pp. 541–558, 2017.

[52] X. Tian, R. R. Negenborn, P. J. van Overloop, J. M. Maestre, A. Sadowska, and N. van de Giesen, "Efficient multi-scenario model predictive control for water resources management with ensemble streamflow forecasts," *Advances in Water Resources*, vol. 109, pp. 58–68, 2017.

[53] F. Pasqualetti, A. Franchi, and F. Bullo, "On cooperative patrolling: Optimal trajectories, complexity analysis, and approximation algorithms," *IEEE Transactions on Robotics*, vol. 28, no. 3, pp. 592–606, 2012.

[54] A. Collins, J. Czyzowicz, L. Gasieniec, A. Kosowski, E. Kranakis, D. Krizanc, R. Martin, and O. Morales Ponce, "Optimal patrolling of fragmented boundaries," in *Proceedings of the Twenty-fifth Annual ACM Symposium on Parallelism in Algorithms and Architectures*. ACM, 2013, pp. 241–250.

[55] R. Kassing, "Model predictive control of open water systems with mobile operators," MSc Thesis, Delft University of Technology, The Netherlands, 2018.

[56] A. M. Williamson, A.-M. Feyer, and R. Friswell, "The impact of work practices on fatigue in long distance truck drivers," *Accident Analysis & Prevention*, vol. 28, no. 6, pp. 709–719, 1996.

[57] E. E. Osuna, "The psychological cost of waiting," *Journal of Mathematical Psychology*, vol. 29, no. 1, pp. 82–105, 1985.

[58] D. A. Hennessy and D. L. Wiesenthal, "Traffic congestion, driver stress, and driver aggression," *Aggressive Behavior*, vol. 25, no. 6, pp. 409–423, 1999.

[59] P. Thiffault and J. Bergeron, "Monotony of road environment and driver fatigue: a simulator study," *Accident Analysis & Prevention*, vol. 35, no. 3, pp. 381–391, 2003.

[60] H. Rakha and Y. Ding, "Impact of stops on vehicle fuel consumption and emissions," *Journal of Transportation Engineering*, vol. 129, no. 1, pp. 23–32, 2003.

[61] M. Mitchell, *An Introduction to Genetic Algorithms*. Cambridge, MA: MIT Press, 1996.

[62] C. Floudas, *Nonlinear and Mixed-Integer Optimization*. Oxford, UK: Oxford University Press, 1995.

[63] I. E. Grossmann and Z. Kravanja, "Mixed-integer nonlinear programming techniques for process systems engineering," *Computers & Chemical Engineering*, vol. 19, pp. 189 – 204, 1995.

[64] F. Fele, J. M. Maestre, S. M. Hashemy, D. M. de la Peña, and E. F. Camacho, "Coalitional model predictive control of an irrigation canal," *Journal of Process Control*, vol. 24, no. 4, pp. 314–325, 2014.

[65] S. Isapoor, A. Montazar, P. J. Van Overloop, and N. Van De Giesen, "Designing and evaluating control systems of the Dez main canal," *Irrigation and Drainage*, vol. 60, no. 1, pp. 70–79, 2011.

[66] A. J. Chipperfield, P. J. Fleming, H. Pohlheim, and C. M. Fonseca, "A genetic algorithm toolbox for matlab," in *Proc. International Conference on Systems Engineering, Coventry, UK*, vol. 6, no. 8, 1994.

[67] A. J. Chipperfield and P. J. Fleming, "The matlab genetic algorithm toolbox," 1995.

[68] P. Wolfe, "The simplex method for quadratic programming," *Econometrica: Journal of the Econometric Society*, pp. 382–398, 1959.

[69] Y. Nesterov and A. Nemirovskii, *Interior-point polynomial algorithms in convex programming*. SIAM, 1994.

[70] D. Greenhalgh and S. Marshall, "Convergence criteria for genetic algorithms," *SIAM Journal on Computing*, vol. 30, no. 1, pp. 269–282, 2000.

[71] Z. Sun, C. Li, J. Zhang, and Y. Xia, "Dynamic event-triggered mpc with shrinking prediction horizon and without terminal constraint," *IEEE Transactions on Cybernetics*, pp. 1–10, 2021.

[72] B. L. Welch, "The Generalization Of 'Student's' Problem When Several Different Population Variances Are Involved," *Biometrika*, vol. 34, no. 1-2, pp. 28–35, 1947.

[73] C. M. Jarque and A. K. Bera, "A test for normality of observations and regression residuals," *International Statistical Review*, vol. 55, no. 2, pp. 163–172, 1987.